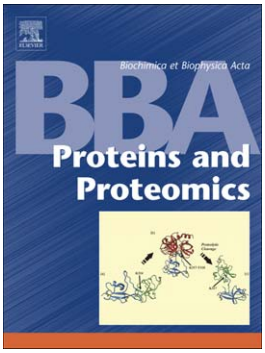

Amyloid fibrils formed by selective N-, C-terminal sequences of mouse apolipoprotein A-II

Jinko Sawashita, Fuyuki Kametani, Kazuhiro Hasegawa, Shinobu Tsutsumi-Yasuhara, Beiru Zhang, Jingmin Yan, Masayuki Mori, Hironobu Naiki, Keiichi Higuchi

PII: S1570-9639(09)00166-6
DOI: doi:10.1016/j.bbapap.2009.06.028
Reference: BBAPAP 38219

To appear in: *BBA - Proteins and Proteomics*

Received date: 12 February 2009
Revised date: 2 June 2009
Accepted date: 26 June 2009

Please cite this article as: Jinko Sawashita, Fuyuki Kametani, Kazuhiro Hasegawa, Shinobu Tsutsumi-Yasuhara, Beiru Zhang, Jingmin Yan, Masayuki Mori, Hironobu Naiki, Keiichi Higuchi, Amyloid fibrils formed by selective N-, C-terminal sequences of mouse apolipoprotein A-II, *BBA - Proteins and Proteomics* (2009), doi:10.1016/j.bbapap.2009.06.028

Amyloid fibrils formed by selective N-, C-terminal sequences of mouse apolipoprotein A-II.

Jinko Sawashita[1*], Fuyuki Kametani[2], Kazuhiro Hasegawa[3], Shinobu Tsutsumi-Yasuhara[3], Beiru Zhang[1, 4], Jingmin Yan[1], Masayuki Mori[1], Hironobu Naiki[3], and Keiichi Higuchi[1]

[1]*Department of Aging Biology, Institute on Aging and Adaptation, Shinshu University Graduate School of Medicine, Matsumoto, Nagano 390-8621, Japan*

[2]*Department of Molecular Neurobiology, Tokyo Institute of Psychiatry, Setagaya-ku, Tokyo 156-8585, Japan*

[3]*Division of Molecular Pathology, Department of Pathological Sciences, Faculty of Medical Science, University of Fukui, Yoshida-gun, Fukui 910-1193, Japan*

[4]*Depertment of Nephrology, Shengjing-Hospital of China Medical University, Shenyang, Liaoning, 110004, China*

[*]Correspondence: Jinko Sawashita, Department of Aging Biology, Institute on Aging and Adaptation, Shinshu University Graduate School of Medicine, 3-1-1 Asahi, Matsumoto, Nagano 390-8621, Japan, Tel. +81 263 37 3392; Fax. +81 263 37 3428; E-mail: jinkos@shinshu-u.ac.jp.

Key words: apolipoprotein A-II, mouse senile amyloidosis, fibril conformation

Financial support: This research was supported in part by a Grant-in-Aid for Young Scientists (B) (15790199) from the Japan Society for the Promotion of Science, by Grants-

24in-Aid for Priority Areas (17028018) and Scientific Research (B) (17390111 and 2520300144) from the Ministry of Education, Culture, Sports, Science and Technology, and 26by a grant to the Amyloidosis Research Committee for the Research on Intractable 27Disease from the Ministry of Health, Labour and Welfare, Japan.

28

29Abbreviations: apoA-I, apolipoprotein A-I; apoA-II, apolipoprotein A-II; AApoAII, 30amyloid fibrils derived from apoA-II; CD, circular dichroism; DMSO, dimethylsulfoxide; 31HDL, high-density lipoprotein; HPLC, high-performance liquid chromatography; LC/MS/ 32MS, liquid chromatography / mass spectrometry / mass spectrometry; LM, light 33microscopy; TEM, transmission electron microscopy; ThT, thioflavin T.

In mice, amyloidogenic type C apolipoprotein A-II (apoA-II) forms amyloid fibrils in age-associated amyloidosis. To understand the mechanism of amyloid fibril formation by apoA-II, we examined the polymerization of synthetic partial peptides of apoA-II in vitro. None of the partial apoA-II peptides polymerized into amyloid fibrils when tested as a single species mixture. We found a unique mechanism in which N- and C-terminal peptides associated into amyloid fibrils in a 1:1 ratio at pH 2.5. The 11-residue amino acid sequence (6-16), which is a common sequence of type B apoA-II and type C apoA-II proteins in amyloidosis-resistant mice and amyloidosis-susceptible mice, respectively, was critical for polymerization into amyloid fibrils. The 18-residue-long amino acid sequence (48-65) is also necessary for nucleation, but not for the extension phase. These findings suggest that there may be different mechanisms underlying the nucleation and extension phases of apoA-II amyloid fibril formation. We also found that amino acid substitutions between type B apoA-II (Pro5, Val38) and type C apoA-II (Gln5, Ala38) did not affect either phase. The strategy of using synthetic partial peptides of amyloidogenic proteins in vitro is a useful system for understanding amyloid fibril formation and for the development of novel therapies.

1. Introduction

In humans and animals, amyloidoses are protein structural disorders characterized by the extracellular deposition of insoluble amyloid fibrils resulting from abnormal conformational changes [1-3]. Amyloid fibrils have a characteristic ultrastructural appearance and a β-pleated-sheets core structure [4] that consists of full length and/or fragments of either wild type or mutant proteins found in familial diseases [5,6]. Several human diseases such as Alzheimer's disease, hemodialysis-associated amyloidosis, prion diseases, and familial amyloid polyneuropathy are associated with amyloid fibril deposition [2,4]. To develop a therapeutic strategy for these disorders, it is essential to understand the mechanisms of amyloid fibril formation. Previous studies have proposed that a nucleation-dependent polymerization model could explain the general mechanisms of amyloid fibril formation in vitro [7-11], but the exact mechanism that converts proteins into amyloid fibrils remains largely unknown.

Apolipoprotein A-II (apoA-II) is the second most abundant apolipoprotein following apolipoprotein A-I (apoA-I) in human and mouse plasma high-density lipoproteins (HDL), composing approximately 20% of the protein mass of human plasma HDL [12-14]. From multiple studies using transgenic mice expressing human or murine apoA-I, apoA-II, or combined apoA-I / apoA-II, it has been shown that apoA-II serves at least two functions; one is to modulate the structure and function of HDL by influencing hepatic lipase in lipolysis, and another is to modulate the anti-inflammatory properties of HDL [13-17]. ApoA-II is also the most important protein associated with mouse senile amyloidosis, as it is the main element of amyloid fibrils (AApoAII) in Senescence-Accelerated Mouse prone 1 (SAMP1) and other strains of mice [18-20]. Seven alleles of

the apoA-II gene have been found among inbred strains of mice with polymorphisms in 15 nucleotide positions comprising 8 amino acid positions [21]. Type C apoA-II protein in amyloidosis-susceptible mice such as SAMP1, contains substitutions of proline (Pro) to glutamine (Gln) at position 5 and of valine (Val) to alanine (Ala) at position 38. Type B apoA-II protein exists in the amyloidosis resistant Senescence-Accelerated Mouse resistant 1 (SAMR1) and other strains of mice [19,22-25]. Genetic analyses using hybrid mice generated from crosses between SAMP1 and SAMR1 mice and congenic and transgenic strains with the type C apoA-II gene (R1.P1-*Apoa2*^{c}, and *Apoa2*^{c}-Tg) have revealed that differences in these amino acids in type C apoA-II are responsible for severe amyloidosis, and Gln at position 5 of type C apoA-II protein might have considerable influence on traits related to the onset of amyloidosis [19,24-26].

Generating 'partial' peptides of amyloidogenic proteins, and analyzing their potential to polymerize into amyloid fibrils have previously provided information about the molecular mechanisms underlying the onset of amyloidoses and also revealed potential target sequence(s) for the prevention of amyloidoses [27-33]. In this study, we evaluate the ability of synthetic mouse apoA-II partial peptides to polymerize in vitro, and found two sequences of apoA-II critical for amyloid fibril formation. We demonstrate that the combination of N- and C-terminal sequences of mouse apoA-II and the conformational change of their secondary structure are essential for polymerization into AApoAII amyloid fibrils, and that different mechanisms may govern nucleation and extension reactions in fibril formation.

2. Materials and methods

2.1. Materials

Synthetic partial peptides (>95.0% purity) of mouse apoA-II shown in **Fig. 1** were obtained from Sigma Genosys (Hokkaido, Japan). For quantitation of peptides in solution, a BCA Protein Assay Reagent Kit was obtained from PIERCE (Illinois, USA). Phosphotungstic acid (electron microscopy grade) was obtained from TAAB Laboratories Equipment Ltd. (Berkshire, England). Other reagents in our experiments were obtained from Wako Pure Chemical Industries, Ltd. (Osaka, Japan). The reaction mixtures for amyloid fibril formation were prepared in 0.5 ml Eppendorf tubes (Safe-Lock tubes, Eppendorf AG, Hamburg, Germany). Carbon-coated grids (400 mesh) for transmission electron microscopy (TEM) were obtained from NEM (Tokyo, Japan), and silanized slide glasses for light microscopy were obtained from DAKO Cytomation Co. (Tokyo, Japan).

2.2. Preparation of Synthetic Peptides Solutions of Mouse ApoA-II

Each synthetic partial peptide was dissolved in 100% dimethylsulfoxide (DMSO) at concentrations of >6 mM, and agitated overnight at 300 rpm at 18˚C in a shaker (Thermomixer Comfort, Eppendorf AG, Hamburg, Germany). The peptide contents of these solutions were determined using a BCA Protein Assay Reagent Kit, and diluted with 100% DMSO to a final concentration of 6 mM. During denaturing treatment with DMSO, amyloid fibril formation was monitored by thioflavin T (ThT) fluorescence [34,35], which did not increase over time. Additionally, the characteristic structures of amyloid fibrils or aggregates were not observed under TEM (data not shown). Aliquots of these peptide solutions were stored in a dark room at 4˚C, and thawed at 20˚C with shaking at 300 rpm for 1 h, and used immediately in each experiment.

2.3. Polymerization of synthetic partial peptides into amyloid fibrils

Reaction mixtures in prechilled tubes contained 50-300 μM synthetic peptide(s), 50 mM reaction buffer, 100 mM NaCl, and 5% DMSO as final concentration. Reaction buffers used were sodium citrate buffer (pH 2.5), sodium acetate buffer (pH 4.5), or sodium phosphate buffer (pH 7.0). After brief blending, the reaction mixtures were incubated with agitation at 300 rpm in a shaker at 37˚C for 0–3 days (up to 13 days maximum), and aliquots were used for ThT binding assays at arbitrary intervals. Furthermore, these mixtures were used for detecting characteristic structures and properties of amyloid fibrils using TEM and LM. The components of amyloid fibrils were analyzed by high-performance liquid chromatography (HPLC) and liquid chromatography / mass spectrometry / mass spectrometry (LC/MS/MS).

2.4. Extension of amyloid fibrils by synthetic partial peptides

The reaction mixtures of synthetic peptides after 4 or 6 days incubation were centrifuged at 1.61×10^4 *g* (1.3×10^4 rpm) at 4˚C for 3 h using a high speed refrigerated microcentrifuge (5415R, Eppendorf AG, Hamburg, Germany), and the supernatants were carefully removed from pellets to avoid contamination with trace quantities of free peptides. Immediately, the amyloid fibril pellets were stored in a –80˚C deep freezer until used as ‘seeds’ for an amyloid fibril extension reaction. The pellets were re-suspended on ice in 50 mM citrate buffer (pH 2.5) containing 100 mM NaCl, and the concentrations of amyloid fibrils in the pellets were measured using a ThT binding assay. These suspensions were sonicated three times on ice for 30 sec at 60-sec intervals using an ultrasonic homogenizer (VP-5S, TAITEC Corporation, Saitama, Japan) at power 4. Reaction mixtures for extension of amyloid fibrils contained 5 μg/ml amyloid fibrils, 50

140μM synthetic peptides, 50 mM citrate buffer (pH 2.5), 100 mM NaCl, and 5% DMSO. 141Reaction mixtures were used for a ThT binding assay, and to determine the structures of 142amyloid fibrils using TEM after incubation.

1432.5. ThT binding assay

144 Endogenous AApoAII amyloid fibrils isolated from livers of mice had optimum ThT-145fluorescence intensities at the excitation and emission wavelengths of 450 nm and 482 nm, 146respectively, with the binding solution containing 250 nM ThT and 50 mM glycine–147NaOH buffer (pH 9.0) at room temperature (22–27˚C) [34,36]. Because the highest 148spectra of ThT-fluorescence intensities of reaction mixtures were 480–484 nm at 149excitation wavelengths of 450 nm in the preliminary tests (data not shown), we performed 150the ThT binding assay under the same conditions used for endogenous AApoAII amyloid 151fibrils with a fluorescence spectrophotometer (RF-5300PC, Shimadzu Corporation, 152Tokyo, Japan). Measurement mixtures were in a total volume of 1 ml, containing 2.5 or 5 153μl aliquots of the reaction mixtures, 250 nM ThT, and 50 mM glycine–NaOH buffer (pH 1549.0). After briefly mixing the solutions at room temperature, the ThT-fluorescence 155intensities were measured. Each reaction mixture was assayed in triplicate, and the 156average was calculated.

1572.6. Microscopic analyses

158 For TEM experiments, the reaction mixtures were spread on carbon-coated grids and 159allowed to stand for 1–2 min before excess solution was removed with filter paper. After 160drying, the grids were negatively stained with 1% phosphotungstic acid–NaOH (pH 7.0), 161incubated briefly, and blotted with filter paper until dry. These samples were examined 162under an electron microscope (1200 EX, JEOL, Tokyo, Japan) with an acceleration

163voltage of 80 kV.

164 For observations under LM, the reaction mixtures were applied on silanized slide 165glasses, dried overnight in a 37˚C dry box, and stained with 1% Congo-red dye in 80% 166ethanol for 30 min. These samples were observed for apple-green color birefringence 167under polarized light using a light microscope (Axioskop 2, Carl Zeiss Japan, Tokyo, 168Japan).

1692.7. LC/MS/MS analysis

170 Aliquots of the reaction mixtures of synthetic peptides were centrifuged at 1.61×10^4 171*g* (1.3×10^4 rpm) at 4˚C for 3 h using a high speed refrigerated microcentrifuge, and the 172pellets were stored in a -80˚C deep freezer immediately after the supernatants were 173removed. The pellets were re-dissolved in 99% formic acid and diluted with 2% formic 174acid / 2% acetonitrile, and analyzed by HPLC and/or LC/MS/MS as described previously 175[37]. The sample solutions were analyzed using the Applied Biosystem HPLC system 176(ABI 140D and ABI 785A). A reverse phase column (C18 column, 0.5 mm i.d. × 150 177mm, Brownlee columns) was used at a flow rate of 5 µl/min with a 10-70% linear gradient 178of acetonitrile in 0.1% trifluoroacetic acid. For LC/MS/MS analysis, the sample solutions 179were applied to a Paradigm MS4 (MicomBioResources, Inc., California, USA) HPLC 180system fitted with an HTC-PAL automatic sampler (CHROMSYS LLC, Virginia, USA). 181A reverse phase capillary column (DevelosilODS-HG5, 0.15 mm i.d. × 50 mm, Nomura 182Chemical Co. Ltd., Aichi, Japan) was used at a flow rate of 2 µl/min with a 4–72% linear 183gradient of acetonitrile in 0.1% formic acid. Eluted apoA-II partial peptides were directly 184detected with ion trap mass spectrometer, LCQ-Advantage (Thermo Electron Corporation, 185Massachusetts, USA). The data were analyzed with SEQUEST (Thermo Electron

186Corporation, Massachusetts, USA).

1872.8. Circular dichroism (CD) analysis

188 Far-UV CD spectra (190–250 nm) of synthetic peptide(s) were measured with a 189spectropolarimeter (J-725, JASCO, Tokyo, Japan) at 25˚C as described previously 190[38,39]. The solutions for spectroscopic measurements contained 50 μM peptide(s), 50 191mM buffer, 100 mM NaCl, and 0.5% hexafluoroisopropanol as final concentrations. 192Buffers used were sodium citrate buffer (pH 2.5), sodium acetate buffer (pH 4.5), or 193sodium phosphate buffer (pH 7.0). To measure the changes in the CD spectra following 194polymerization of the synthetic peptides, the CD spectra of N- and C-terminal peptides 195(c16p + 48/65) were first recorded within 5 min after mixing these peptides in the solution 196(immediate phase). Then, peptide solutions were subsequently incubated for 197approximately 12 h at 37˚C, and their CD spectra were recorded (overnight phase). Five 198consecutive readings at a bandwidth of 1 nm, a response time of 1 sec, and a resolution of 1990.2 nm were taken from each sample and averaged, baseline-subtracted, and noise-200reduced. The CD signals were recorded in a 1 mm path length quartz cell. Results were 201expressed in terms of mean residue ellipticity (MRE).

202**3. Results**

2033.1. Polymerization of synthetic partial peptides into amyloid fibrils

204 We examined fibril formation of synthetic partial peptides of mouse apoA-II in vitro 205(**Fig. 1**). ThT-fluorescence intensities of the reaction mixtures containing 50 μM of N- 206and C-terminal peptides (c16p + 48/65) were stable up to 1 h of incubation at pH 2.5, and 207then increased until they reached a plateau phase after 6 h (**Fig. 2A**). Abundant amyloid 208fibrils with characteristic structures were observed in these reaction mixtures after 21 h 209and 3 days incubation at pH 2.5 using TEM, and apple-green birefringence was observed 210in the mixture stained with Congo-red under polarizing LM (**Fig. 2B** and **Supplementary** 211**Fig. S1A**). HPLC and LC/MS/MS analysis revealed that amyloid fibrils formed in the 212reaction mixture containing c16p and 48/65 had both peptides in a 1:1 ratio (**Fig. 2C**). 213When c16p + 48/65 mixtures were incubated at pH 4.5 or 7.0, ThT-fluorescence 214intensities increased less than the intensities at pH 2.5 (**Fig. 2A**, **2B** and **Supplementary** 215**Fig. S2**). The fluorescence intensities of the reaction mixtures containing solely c16p or 21648/65 were relatively unchanged even after 24 h incubation at a higher concentration of 217300 μM at pH 2.5 (**Fig. 2A**). None of the synthetic peptides shown in **Fig. 1** polymerized 218into amyloid fibrils when used as a single species mixture (data not shown).

219 To further study the amyloid fibril formation in acidic conditions, we measured the 220far-UV CD spectra of c16p and 48/65 peptides within 5 min (immediate phase) after 221mixing them at pH 2.5 (**Fig. 3**). The CD spectrum of c16p alone (c16p) exhibited one 222negative peak at 200 nm, and that of 48/65 alone (48/65) exhibited one negative peak at 223216-222 nm following a typical pattern of β-structure and β-turn. The CD spectrum of the 224mixture of these peptides (c16p + 48/65) showed almost the same shape as that of the

c16p alone rather than the merged spectrum of each c16p and 48/65 peptides. The CD spectrum of c16p + 48/65 after incubation at pH 2.5 for 12 h at 37˚C (overnight phase) changed greatly and exhibited one broad and negative peak at 216 nm (**Fig. 3A**). The CD spectra of c16p + 48/65 in immediate phase and overnight phase at pH 4.5 and 7.0 showed different confirmations from those at pH 2.5 (**Fig. 3B**).

Higuchi and co-workers suggested the important contribution of the N-terminus of apoA-II to amyloid fibril formation from the greater amyloidogenicity of pro-apoA-II with 25-extra-amino acids at N-terminus and type C apoA-II protein with Gln at position 5 from N-terminus [22,40]. We compared the polymerization characteristics of a propeptide c16p with several N-terminal c16p deletions (**Fig. 4**). First, we examined the polymerization of N-terminal deletions. ThT-fluorescence intensities of the reaction mixtures of c1/16 without a propeptide and 48/65 (c1/16 + 48/65) increased as did the intensities of the reaction mixture of c16p with propeptide (c16p + 48/65) (**Fig. 4A**). Reaction mixtures of N-terminal deletions (c2/16 or 6/16) showed increased intensities almost the same as those of c1/16. We detected the characteristic structure of amyloid fibrils using TEM in the reaction mixtures of N-terminal deletions, but the fluorescence intensities of 9/16 without amino acids at position 1–8 of N-terminal peptide increased only slightly, and the characteristic structure of amyloid fibrils was not detected (**Fig. 4A** and **4E**). Secondly, we examined polymerization of N-terminal deletions with a C-terminal deletion. In general, it has been believed that Gln is an amyloidogenic amino acid, and that Pro is a β-sheet breaker [41-45]. We found that ThT-fluorescence intensities of reaction mixtures of short N-terminal peptides whose C-terminal was Gln at position 8 or 13 (c8p or c13p, respectively) increased much less compared with the intensities of the reaction mixture of

248c16p with Gln at position 16 (**Fig. 4B**). The fluorescence intensities of the reaction
249mixture of c15p without Gln at position 16 did not increase, and the characteristic
250structure of amyloid fibrils could not be detected (**Fig. 4C** and **4E**). The fluorescence
251intensities of the reaction mixture of c1/16(Q16H) having histidine (His) substituted for
252Gln at position 16 were sharply reduced from the intensities of the reaction mixture of
253c1/16. Only a small number of amyloid fibril-like structures were detected in the reaction
254mixture.

255 Furthermore, the fluorescence intensities of the reaction mixture of 16/6 + 65/48
256combination, which were synthesized as peptides with inverse sequences in comparison
257with 6/16 or 48/65 peptides, increased much less compared with that of 6/16 + 48/65
258combination, and the characteristic structure of amyloid fibrils could not be detected (**Fig.**
259**4D** and **4E**). The fluorescence intensities of the reaction mixtures of those peptides with
260inverse sequences (16/6 or 65/48) were also unchanged even though they coexisted with
261peptides with native sequences (48/65 or 6/16, respectively).

262 In previous in vivo studies, we suggested that differences in amino acids, in particular
263Gln at position 5 of type C apoA-II protein, have considerable influence on
264amyloidogenesity of apoA-II protein [19,24,25]. In light of these observations, we
265examined polymerization of the N-terminal peptide (b16p) of type B apoA-II with Pro at
266position 5 (**Fig. 5**). ThT-fluorescence intensities of the reaction mixture containing b16p
267and 48/65 were stable up to 1 h of incubation at pH 2.5, and then increased until they
268reached a plateau phase after 6 h (**Fig. 5A** and **Supplementary Fig. S1B**). There was no
269difference in the kinetics of amyloid fibril formation between c16p (**Fig. 2A**) and b16p.
270ThT-fluorescence intensities increased only slightly after incubation at pH 4.5 and 7.0.

Abundant amyloid fibrils with characteristic structures were observed in the reaction mixtures of b16p at pH 2.5 using TEM, and apple-green birefringence was observed in the mixture stained with Congo-red under polarizing LM (**Fig. 5B** and **Supplementary Fig. S1B**).

Next, we examined the polymerization of three C-terminal deletions containing partial sequences of 48/65 and another C-terminal peptide 64/78. ThT-fluorescence intensities of the reaction mixtures of c16p and each C-terminal peptide(s) (48/57, 52/61, 56/65, 48/57 + 56/65) demonstrated a limited increase compared with the intensities of c16p + 48/65 mixture (**Fig. 6A**).

Finally, we also examined peptides with an amino acid substitution at position 38 found between type B and C apoA-II. The fluorescence intensities of the reaction mixtures of the middle part peptide (c32/43) and either c16p or 48/65 (c16p + c32/43 or 48/65 + c32/43) did not increase compared with the intensities of the mixture containing both c16p and 48/65 (c16p + 48/65) (**Fig. 6B**). The fluorescence intensities of the reaction mixtures of N-terminal peptides (c16p or b16p), 48/65, and mid-section peptides (c32/43 or b32/43) increased greatly, similar to the intensities of N-terminal peptides and 48/65 without mid-section peptides (**Fig. 6B** and **6C**).

3.2. Extension of amyloid fibrils by synthetic partial peptides

We investigated the extension of amyloid fibrils with synthetic peptides when pre-made amyloid fibrils were added in the reaction mixture as seeds. Amyloid fibrils were collected as pellets following centrifugation of the reaction mixtures containing amyloid fibrils made from N- and C-terminal peptides. With the pre-made amyloid fibrils derived from type C peptides (c16p + 48/65) in the reaction mixtures, the fluorescence intensities

of the reaction mixtures of N-terminal peptides (c16p or c1/16) increased rapidly from the beginning of incubation and reached a plateau phase after approximately 2 h (**Fig. 7A**). The lag-time phase shown in **Fig. 2A** disappeared with the pre-made amyloid fibrils in the reaction mixtures (**Fig. 7A** right panel). The fluorescence intensities of the reaction mixture of type B N-terminal peptide (b16p) increased in almost the same pattern as the intensities of type C N-terminal peptides (c16p). The fluorescence intensities of type C N-terminal peptides without a Gln at position 16 (c8p or c13p) did not increase. With the addition of the pre-made amyloid fibrils derived from type B peptides (b16p + 48/65), the fluorescence intensities of the reaction mixtures of either type B (b16p) or type C (c16p) peptide increased rapidly without a lag-time phase (**Fig. 7B**). The patterns of fluorescence intensities were similar to the patterns obtained with type C pre-made amyloid fibrils shown in **Fig. 7A**.

The fluorescence intensities of the reaction mixture containing the c16p peptide alone gradually increased when pre-made amyloid fibrils were added, whilst the intensities of the 48/65 peptide alone did not increase (**Fig. 7C**). Using TEM, we examined the structure of amyloid fibrils in the reaction mixtures of c16p and 48/65 peptides over a 3 days period with pre-made amyloid fibrils using TEM (**Fig. 7D**). We observed characteristic amyloid fibrils with structures similar to amyloid fibrils obtained without seeds. In the reaction mixtures of c16p peptide without 48/65 peptide, we observed narrower and curving amyloid fibril structures after 3 days of incubation with pre-made amyloid fibrils. The reaction mixtures of only the 48/65 peptide incubated for 3 days with pre-made amyloid fibrils had no amyloid fibrils.

4. Discussion

In order to investigate the mechanism of amyloid fibril formation from apoA-II in mouse senile amyloidosis, we examined the fibril formation in vitro using various synthetic peptides. We also designed peptides to investigate the role of amino acid substitutions found between type C apoA-II of amyloidosis-susceptible mice and type B apoA-II of amyloidosis-resistant mice.

When used alone, none of the individual synthetic peptides shown in **Fig. 1** polymerized into amyloid fibrils in the reaction conditions we tried. However, a combined mixture of c16p and 48/65 peptides polymerized into amyloid fibrils constituted of both peptides. The increase in ThT-fluorescence intensities followed a typical sigmoidal pattern. The fluorescence intensities were stable for up to 1 h of incubation (the nucleation phase), then increased linearly, and reached a plateau phase after 6 h (the extension phase). Adding pre-made amyloid fibrils eliminated the nucleation phase, and led to an earlier plateau phase. From these results, we conclude that the N- and C-terminal peptides of apoA-II polymerize according to the "nucleation-dependent polymerization model" described for various amyloid proteins [8,9,46] and type C natural apoA-II [47]. This novel finding that two peptides with different properties cooperate to polymerize into amyloid fibrils, may shed new light on the molecular mechanisms of amyloid fibril formation.

In the presence of pre-made amyloid fibrils of c16p + 48/65, the ThT-fluorescence intensities of the reaction mixtures containing the N-terminal c16p peptide increased even without the C-terminal 48/65 peptide. However, the amyloid fibrils were narrower and more bent compared to c16p + 48/65 amyloid fibrils. The fluorescence intensities of the

339reaction mixtures of c16p and 48/65 in a 5:1 ratio showed an extended lag-time phase up
340to 3 h, and then increased until 3 days (**Supplementary Fig. S3A**). LC/MS/MS analysis
341revealed that the ratios of c16p and 48/65 peptides in amyloid fibrils were 2:1 and 5:1
342after 21 h and 3 days of incubation, respectively (**Supplementary Fig. S3B**).
343Furthermore, TEM analysis of the products from these reactions revealed the same narrow
344and bent amyloid fibrils (**Supplementary Fig. S3C**). C16p might polymerize to nuclei
345and fibrils in cooperation with 48/65 initially, then, extend fibrils after the 48/65 peptide
346was exhausted. These results suggest that different mechanisms might exist between the
347nucleation and extension phases of amyloid fibril formation of apoA-II, and that the C-
348terminal peptide may be indispensable for the nucleation, but not for the extension phase.

349 We previously reported that pro-apoA-II with a 5-residue-long propeptide had greater
350amyloidogenicity than mature apoA-II [22,40]; therefore we examined polymerization of
351peptides with N-terminal deletions. ThT-fluorescence intensities of reaction mixtures
352containing the c1/16 without the propeptide sequence and 48/65 peptides increased
353similarly to those containing propeptide c16p and 48/65 peptides. This result suggests that
354the propeptide sequence at least in vitro might not play an important role in the
355polymerization of apoA-II protein.

356We examined the effects of pH on polymerization of synthetic partial peptides of apoA-II.
357Under weak-acidic (pH 4.5) or neutral (pH 7.0) conditions, ThT-fluorescence intensities
358of c16p and 48/65 peptides increased less than the intensities in an acidic (pH 2.5)
359condition, although a smaller number of similarly shaped amyloid fibrils was observed.
360We measured the far-UV CD spectra of c16p and 48/65 peptides under immediate and
361overnight phase at pH 2.5, and found the conformational change of c16p + 48/65 mixture.

362Previous studies conclude that amyloid-associated proteins such as immunoglobulin light
363chain (AL amyloidosis), serum AA (AA amyloidosis), and apoA-I (AApoAI amyloidosis)
364need to change into unstable and β-sheet rich structure in order to form into amyloid
365fibrils [48,49]. Under acidic conditions, we believe that it is necessary for the unfolded
366intermediate structure of 48/65 peptide to cooperate with the c16p peptide before the final
367conformational change of c16p and 48/65 peptides to amyloid fibrils. It is possible that
368these acidic in vitro experiments recapitulate the in vivo setting where the low pH of the
369lysosome dramatically affects amyloid fibril formation. One possibility is that denaturing
370of apoA-II in lysosome precedes amyloid fibril formation, although we have not found
371that AApoAII amyloid fibrils deposit in lysosome [20,24,40,47]. Our colleagues found
372that β2-microglobulin, like apoA-II peptides, not only forms amyloid fibrils under low pH
373(pH 2.5), but easily forms amyloid fibrils at neutral pH in the presence of heparin or
374several phospholipids [39,50]. In our preliminary experiments, the polymerization of
375c16p and 48/65 peptides of apoA-II could be enhanced at pH 7.0 in the presence of
376heparin, heparane sulfate, or proteoglycans (data not shown). Thus, undetermined
377extracellular components might enhance the amyloid fibril formation of natural apoA-II at
378neutral pH in vivo. In order to test this hypothesis, we must find the molecular
379mechanisms of the interaction of apoA-II and the extracellular components.

380 Gln is well known as an amyloidogenic amino acid [43-45,51], and c16p peptide
381contains Glns at 5 positions (1, 5, 8, 13 and 16; **Fig. 1**). We studied the contribution of
382these Gln to polymerization using shorter peptides with N- and C-terminal c16p
383deletions. These results indicate that Gln at positions 8 and 13 play an indispensable role
384in amyloid fibril formation. Furthermore the substitution of Gln to His in the

385c1/16(Q16H) peptide inhibited polymerization. This indicates that the 11-residue peptide
386corresponding to amino acids 6–16 of apoA-II is a “core” peptide. Interestingly, ThT-
387fluorescence intensities of reaction mixtures containing c16p with C-terminal deletion
388peptide(s) of 48/65 (48/57, 52/61, 56/65, and 48/57 + 56/65) and the C-terminal peptide
38964/78 did not increase polymerization. This result suggests that the 18-residue-long
390peptide of 48/65 is necessary for polymerization. Furthermore, peptides with reverse-
391sequences (16/6 or 65/48) could not polymerize to amyloid fibrils even with forward
392(native) peptides (48/65 or 6/16, respectively) at pH 2.5. Equally, a combination of 16/6
393and 65/48 could not polymerize to amyloid fibrils. These results suggest that sequences of
394N- and C-terminal regions are essential for the polymerization to amyloid fibrils, not
395components of them.

396 We previously reported that Gln at position 5 might be a key amino acid for
397polymerization of type C apoA-II [19,23,24,52]. However, here we found that the type B
398peptide (b16p) with Pro at position 5 had the same properties as c16p in the nucleation and
399extension phases and formed amyloid fibrils with a similar seeding ability and structure as
400amyloid fibrils made from c16p under acidic (pH 2.5) conditions. We did not find a
401difference between c16p and b16p even when they were incubated with the 48/65 at pH
4024.5 or 7.0. These results suggest that Gln at position 5 might not be an important amino
403acid for polymerization under the conditions described here. Our previous report found
404that type B apoA-II acted as an active inhibitor of amyloid fibril extension of type C
405apoA-II in vivo [53]. Genetic analyses suggested that the ability of type B apoA-II to
406increase cholesterol levels was due to an Ala to Val substitution at position 38 [54]. Thus,
407we examined the contribution of interior peptides with a substitution at position 38

(c32/43 and b32/43) to the polymerization of apoA-II. Addition of c32/43 or b32/43 peptides in the reaction mixture of N-terminal (c16p or b16p) and C-terminal (48/65) peptides did not alter the polymerization at pH 2.5. LC/MS/MS analysis of amyloid fibrils made in reaction mixtures of c16p, 48/65 and c32/43 after 3 days of incubation at pH 2.5 did not contain c32/43 (data not shown). These data imply that the substitution at position 38 between type B and C apoA-II may not contribute to the different amyloidogenicity observed between type B and C apoA-II. It is remarkable that an amyloidogenic property of type B apoA-II is identical with that of type C apoA-II in vitro, but it remains unclear why mice with type B apoA-II are amyloidosis-resistant. We cannot explain the different in the in vitro and in vivo mechanisms of type B apoA-II. Mouse apoA-II proteins probably generate surface patches that associate with acyl side chains of lipids in serum HDL similar to human apoA-II [55]. We have found that amount and particle size of plasma HDL on SAMR1 mice with type B apoA-II were greater and larger compared with those of R1.P1-*Apoa2*^{c} congenic mice with type C apoA-II [26]. This R1.P1-*Apoa2*^{c} congenic mouse strain was developed in our laboratory, and had the identical genetic background with SAMR1 mice except for type C apoA-II. We expect that Type B apoA-II may differ from type C apoA-II in binding affinity with lipids of HDL and its role in metabolic processes. We have also found that intravenous injection of AApoAII amyloid fibrils of type C apoA-II into SAMR1 mice with type B apoA-II can induce senile amyloidosis, and new AApoAII amyloid fibrils obtained from the amyloidosis-induced SAMR1 mouse can cause earlier and more severe amyloidosis in SAMR1 mice than AApoAII of type C apoA-II [25]. So we believe that senile amyloidosis is easily induced in mice with type B apoA-II by simply changing the microenvironment into an unknown

pathogenic state.

We hypothesize a unique model for the AApoAII amyloid fibril formation obtained in our studies using synthetic partial peptides (**Fig. 8**). The model contains elements from "the nucleation-dependent polymerization model," which consists of nucleation and extension phases, as well as the amyloid fibril formation model for prion protein [9], amyloid β-protein [7,46], and β2-microglobulin [8]. The combination of N- and C-terminal regions of apoA-II is essential for their association into nuclei of amyloid fibrils, and once the nucleus has been formed, further addition of N- and C-terminal peptides is accelerated. Interestingly, in the presence of "nuclei or seeds," the N-terminal peptide polymerized into amyloid fibrils even without the C-terminal peptide, but these fibrils were narrower and more bent than those formed from both the N- and C-terminal peptides.

Based on these findings in vitro, we hypothesize an in vivo mechanism of polymerization into amyloid fibrils shown in **Fig. 8B**. Some apoA-II proteins separate from the lipid surface, form the unfolded intermediate structure and associate to nucleus (nucleation phase). The unfolded apoA-II binds to nucleus and extends amyloid fibrils (AApoAII; the extension phase). When exogenous AApoAII amyloid fibrils are ingested, they act as seeds to induce and stabilize conversion of apoA-II protein. This mechanism provides a plausible explanation for the transmission of AApoAII amyloidosis [56]. It is not clear whether the extension phase progresses through the combination of N- and C-sequences of apoA-II or N-terminal sequence alone, but narrow and bending forms of amyloid fibrils were not observed in the tissues of mice with type C apoA-II [25,36].

The molecular mechanism underlying the different amyloidogenesis processes in type

454B and C apoA-II mice with amino acid mutations Pro5Gln and Ala38Val, could not be
455elucidated in our in vitro studies. Yanagisawa and other researchers have suggested that
456each Aβ-protein with different mutations in hereditary Alzheimer's disease, selects
457specific sialoglycolipids on the cell membrane surface to interact and extend amyloid
458fibrils [57-61]. Other researchers have suggested that phospholipids contribute to
459stabilization of apoA-I [49] and α-synuclein [62]. We hypothesize that amino acid
460substitutions between type C and B apoA-II may alter the ability to interact with target
461molecules such as cholesterols, phospholipids, glycolipids, and proteins in some
462microenvironments and lead to different amyloidogenesity.

463 Our in vitro study using synthetic partial peptides of mouse apoA-II revealed a unique
464mechanism for mouse AApoAII amyloid fibril formation. This polymerization requires a
465combination of N- and C-terminal sequences of mouse apoA-II and acidity (pH 2.5). The
466strategy using synthetic partial peptides is useful and simple for understanding various
467issues in amyloidosis, including the mechanism of amyloid fibril formation, cell toxicity,
468and transmission. But we need to demonstrate the mechanism for polymerization using a
469full-length peptide of apoA-II. Further investigations using partial and full-length
470peptides may elucidate the mechanisms of AApoAII and other general amyloidoses.

471**Acknowledgements**

472 We thank Mr. Kiyokazu Kametani and Ms. Kayo Suzuki (Research Support Center for 473Human and Environmental Sciences, Shinshu University, Nagano, Japan) for technical assistance 474of TEM.

475 Financial support: This research was supported in part by a Grant-in-Aid for Young 476Scientists (B) (15790199) from the Japan Society for the Promotion of Science, by Grants-in-Aid 477for Priority Areas (17028018) and Scientific Research (B) (17390111 and 20300144) from the 478Ministry of Education, Culture, Sports, Science and Technology, and by a Grant-in-Aid for the 479Intractable Disease Division, the Ministry of Health Labour and Welfare to Research Committees 480for Amyloidosis and a Research Committee for Epochal Diagnosis and Treatment of Amyloidosis 481in Japan.

References

[1] P. Westermark, The pathogenesis of amyloidosis, Am. J. Pathol. 152 (1998) 1125-1127.

[2] P. Westermark, M.D. Benson, J.N. Buxbaum, A.S. Cohen, B. Frangione, S. Ikeda, C.L. Masters, G. Merlini, M.J. Saraiva, J.D. Sipe, Amyloid fibril protein nomenclature – 2002, Amyloid 9 (2002) 197-200.

[3] J.P. Taylor, J. Hardy, K.H. Fischbeck, Toxic proteins in neurodegenerative disease, Science 296 (2002) 1991-1995.

[4] M. Stefani, C.M. Dobson, Protein aggregation and aggregate toxicity: new insights into protein folding, misfolding diseases and biological evolution, J. Mol. Med. 81 (2003) 678-699.

[5] M. Yazaki, J. Varga, J.B. Dyck, M.D. Benson, A new transthyretin variant Leu55Gln in a patient with systemic amyloidosis, Amyloid 9 (2002) 268-271.

[6] D.J. Selkoe, Cell biology of protein misfolding: the examples of Alzheimer's and Parkinson's diseases, Nat. Cell Biol. 6 (2004) 1054-1061.

[7] K. Hasegawa, I. Yamaguchi, S. Omata, F. Gejyo, H. Naiki, Interaction between Aβ(1-42) and Aβ(1-40) in Alzheimer's β-amyloid fibril formation *in vitro*, Biochem. 38 (1999) 15514-15521.

[8] G.V. Kozhukh, Y. Hagihara, T. Kawakami, K. Hasegawa, H. Naiki, Y. Goto, Investigation of a peptide responsible for amyloid fibril formation of β_2-microgloblin by Achromobacter protease I, J. Biol. Chem. 277 (2002) 1310-1315.

[9] A.J. Modler, H. Fabian, F. Sokolowski, G. Lutsch, K. Gast, G. Damaschun, Polymerization of proteins into amyloid protofibrils shares common critical oligomeric states but differs in the mechanisms of their formation, Amyloid 11 (2004) 215-231.

[10] R.A. Kammerer, D. Kostrewa, J. Zurdo, A. Detken, C. Garcia-Echeverria, J.D. Green, S.A. Müller, B.H. Meier, F.K. Winkler, C.M. Dobson, M.O. Steinmetz, Exploring amyloid

507 formation by a de novo design, Proc. Natl. Acad. Sci. USA 101 (2004) 4435-4440.

508[11] H.D. Nguyen, C.K. Hall, Kinetics of fibril formation by polyalanine peptides, J. Biol.
509 Chem. 280 (2005) 9074-9082.

510[12] G.M. Kostner, D.R. Patsch, S. Sailer, H. Braunsteiner, A. Holasek, Polypeptide distribution
511 of the main lipoprotein density classes separated from human plasma by rate zonal
512 ultracentrifugation, Eur. J. Biochem. 45 (1974) 611-621.

513[13] J.R. Schultz, E.L. Gong, M.R. McCall, A.V. Nichols, S.M. Clift, E.M. Rubin, Expression of
514 human apolipoprotein A-II and its effect on high density lipoproteins in transgenic mice, J.
515 Biol. Chem. 267 (1992) 21630-21636.

516[14] E.L. Gong, L.J. Stoltzfus, C.M. Brion, D. Murugesh, E.M. Rubin, Contrasting *in vivo*
517 effects of murine and human apolipoprotein A-II, J. Biol. Chem. 271 (1996) 5984-5987.

518[15] C.H. Warden, A. Daluiski, X. Bu, D.A. Purcell-Huynh, C. De Meester, B.H. Shieh, D.L.
519 Puppione, R.M. Gray, G.M. Reaven, Y.D. Chen, J.I. Rotter, A.J. Lusis, Evidence for
520 linkage of the apolipoprotein A-II locus to plasma apolipoprotein A-II and free fatty acid
521 levels in mice and humans, Proc. Natl. Acad. Sci. USA 90 (1993) 10886-10890.

522[16] P. Holvoet, S. Danloy, E. Deridder, M. Lox, H. Bernar, A. Dhoest, D. Collen, Substitution
523 of the carboxyl-terminal domain of apo AI with apo AII sequences restores the potential of
524 HDL to reduce the progression of atherosclerosis in apo E knockout mice, J. Clin. Invest.
525 102 (1998) 379-385.

526[17] C.C. Hedrick, L.W. Castellani, H. Wong, A.J. Lusis, *In vivo* interactions of apoA-II, apoA-I,
527 and hepatic lipase contributing to HDL structure and antiatherogenic functions, J. Lipid Res.
528 42 (2001) 563-570.

529[18] K. Higuchi, T. Yonezu, K. Kogishi, A. Matsumura, S. Takeshita, K. Higuchi, A. Kohno, M.
530 Matsushita, M. Hosokawa, T. Takeda Purification and characterization of a senile amyloid-
531 related antigenic substance (apoSAS$_{SAM}$) from mouse serum, J. Biol. Chem. 261 (1986)

12834-12840.

[19] K. Higuchi, T. Yonezu, S. Tsunasawa, F. Sakiyama, T. Takeda, The single proline-glutamine substitution at position 5 enhances the potency of amyloid fibril formation of murine apoA-II, FEBS Lett. 207 (1986) 23-27.

[20] K. Higuchi, H. Naiki, K. Kitagawa, M. Hosokawa, T. Takeda, Mouse senile amyloidosis; AS_{SAM} amyloidosis in mice presents universally as a systemic age-associated amyloidosis, Virchows Arch. B Cell Pathol Incl. Mol. Pathol. 60 (1991) 231-238.

[21] K. Kitagawa, J. Wang, T. Matsushita, K. Kogishi, M. Hosokawa, X. Fu, Z. Guo, M. Mori, K. Higuchi, Polymorphisms of mouse apolipoprotein A-II: seven alleles found among 41 inbred strains of mice, Amyloid 10 (2003) 207-214.

[22] T. Yonezu, S. Tsunasawa, K. Higuchi, K. Kogishi, H. Naiki, K. Hanada, F. Sakiyama, T. Takeda, A molecular-pathologic approach to murine senile amyloidosis: Serum precursor-apoA-II variant (Pro^5-Gln) presents only in the senile amyloidosis prone SAM-P/1 and SAM-P/2 mice, Lab. Invest. 57 (1987) 65-70.

[23] K. Higuchi, K. Kitagawa, H. Naiki, K. Hanada, M. Hosokawa, T. Takeda, Polymorphism of apolipoprotein A-II (apoA-II) among inbred strains of mice. Relationship between the molecular type of apoA-II and mouse senile amyloidosis, Biochem. J. 279 (1991) 427-433.

[24] K. Higuchi, K. Kogishi, J. Wang, X. Chen, T. Chiba, T. Matsushita, Y. Hoshii, H. Kawano, T. Ishihara, T. Yokota, M. Hosokawa, Fibrilization in mouse senile amyloidosis is fibril conformation-dependent, Lab. Invest. 78 (1998) 1535-1542.

[25] Y. Xing, A. Nakamura, T. Korenaga, Z. Guo, J. Yao, X. Fu, T. Matsushita, K. Kogishi, M. Hosokawa, F. Kametani, M. Mori, K. Higuchi, Induction of protein conformational change in mouse senile amyloidosis, J. Biol. Chem. 277 (2002) 33164-33169.

[26] F. Ge, J. Yao, X. Fu, Z. Guo, J. Yan, B. Zhang, H. Zhang, H. Tomozawa, J. Miyazaki, J. Sawashita, M. Mori, K. Higuchi, Amyloidosis in transgenic mice expressing murine

557 amyloidogenic apolipoprotein A-II (*Apoa2*^{c}), Lab. Invest. 87 (2007) 633-643.

558[27] J.A. Palha, D. Ballinari, N. Amboldi, I. Cardoso, R. Fernandes, V. Bellotti, G Merlini, M.J.
559 Saraiva, 4'-Iodo-4'-deoxydoxorubicin disrupts the fibrillar structure of transthyretin
560 amyloid, Am. J. Pathol. 156 (2000) 1919-1925.

561[28] C. Korth, B.C. May, E.E. Cohen, S.B. Prusiner, Acridine and phenothiazine derivatives as
562 pharmacotherapeutics for prion disease, Proc. Natl. Acad. Sci. USA 98 (2001) 9836-9841.

563[29] J. McLaurin, R. Cecal, M.E. Kierstead, X. Tian, A.L. Phinney, M. Manea, J.E. French,
564 M.H. Lambermon, A.A. Darabie, M.E. Brown, C. Janus, M.A. Chishti, P. Horne, D.
565 Westaway, P.E. Franser, H.T. Mount, M. Przybylski, St. P. George-Hyslop, Therapeutically
566 effective antibodies against amyloid-β peptide target amyloid-β residues 4-10 and inhibit
567 cytotoxicity and fibrillogenesis, Nat. Med. 8 (2002) 1263-1269.

568[30] K. Ono, K. Hasegawa, Y. Yoshiike, A. Takashima, M. Yamada, H. Naiki,
569 Nordihydroguaiaretic acid potently breaks down pre-formed Alzheimer's β-amyloid fibrils
570 *in vitro*, J. Neurochem. 81 (2002) 434-440.

571[31] K.P. Townsend, D. Praticò, Novel therapeutic opportunities for Alzheimer's disease: focus
572 on nonsteroidal anti-inflammatory drugs, FASEB J. 19 (2005) 1562-1601.

573[32] D. Frenkel, R. Maron, D.S. Burt, H.L. Weiner, Nasal vaccination with a proteosome-based
574 adjuvant and glatiramer acetate clears β-amyloid in a mouse model of Alzheimer disease, J.
575 Clin. Invest. 23 (2005) 462-469.

576[33] N.S. Green, T.R. Foss, J.W. Kelly, Genistein, a natural product from soy, is a potent
577 inhibitor of transthyretin amyloidosis, Proc. Natl. Acad. Sci. USA 102 (2005) 14545-15550.

578[34] H. Naiki, K. Higuchi, M. Hosokawa, T. Takeda, Fluorometric determination of amyloid
579 fibrils *in vitro* using the fluorescent dye, thioflavine T, Anal. Biochem. 177 (1989) 244-249.

580[35] T. Ban, D. Hamada, K. Hasegawa, H. Naiki, Y. Goto, Direct observation of amyloid fibril
581 growth monitored by thioflavin T fluorescence, J. Biol. Chem. 278 (2003) 16462-16465.

582[36] T. Korenaga, X. Fu, Y. Xing, T. Matsusita, K. Kuramoto, S. Syumiya, K. Hasegawa, H.
583 Naiki, M. Ueno, T. Ishihara, M. Hosokawa, M. Mori, K. Higuchi, Tissue distribution,
584 biochemical properties, and transmission of mouse type A AApoAII amyloid fibrils, Am. J.
585 Pathol. 164 (2004) 1597-1606.
586[37] F. Kametani, Secretion of long Aβ-related peptides processed at ε-cleavage site is
587 dependent on the α-secretase pre-cutting, FEBS Lett. 570 (2004) 73-76.
588[38] S. Yamamoto, K. Hasegawa, I. Yamaguchi, S. Tsutsumi, J. Kardos, Y. Goto, F. Gejyo, H.
589 Naiki, Low concentrations of sodium dodecyl sulfate induce the extension of β_2-
590 microglobulin-related amyloid fibrils at a neutral pH, Biochem. 43 (2004) 11075-11082.
591[39] S. Yamamoto, I. Yamaguchi, K. Hasegawa, S. Tsutsumi, Y. Goto, F. Gejyo, H. Naiki,
592 Glycosaminoglycans enhance the trifluoroethanol-induced extension of β_2-microglobulin-
593 related amyloid fibrils at a neutral pH, J. Am. Soc. Nephrol. 15 (2004) 126-133.
594[40] K. Higuchi, K. Kogishi, J. Wang, C. Xia, T. Chiba, T. Matsushita, M. Hosokawa,
595 Accumulation of pro-apolipoprotein A-II in mouse senile amyloid fibrils, Biochem. J. 325
596 (1997) 653-659.
597[41] S.J. Wood, R. Wetzel, J.D. Martin, M.R. Hurle, Prolines and amyloidogenicity in fragments
598 of the Alzheimer's peptide beta/A4, Biochem. 34 (1995) 724-730.
599[42] C. Soto, E.M. Sigurdsson, L. Morelli, R.A. Kumar, E.M. Castaño, B. Frangione, β-sheet
600 breaker peptides inhibit fibrillogenesis in a rat brain model of amyloidosis: implications of
601 Alzheimer's therapy, Nat. Med. 4 (1998) 822-826.
602[43] S.H. Satyal, E. Schmidt, N. Sondheimer, S. Lindquist, J.M. Kramer, R. Morimoto,
603 Polyglutamine aggregates alter protein folding homeostasis in Caenorhabditis elegans, Proc.
604 Natl. Acad. Sci. USA 97 (2000) 5750-5755.
605[44] M.F. Perutz, B.J. Pope, E.E. Wanker, E. Scherzinger, Aggregation of proteins with
606 expanded glutamine and alanine repeats of the glutamine-rich and asparagine-rich domains

607 of Sup35 and of the amyloid β-peptide of amyloid plaques, Proc. Natl. Acad. Sci. USA 99
608 (2002) 5596-5600.
609[45] I.L. Derkatch, S.M. Uptain, T.F. Outerio, R. Krishnan, S.L. Lindquist, S.W. Liebman,
610 Effects of Q/N-rich, polyQ, and non-polyQ amyloids on the de novo formation of the [PSI^+]
611 prion in yeast and aggregation of Sup35 *in vitro*, Proc. Natl. Acad. Sci. USA 101 (2004)
612 12934-12939.
613[46] J.T. Jarrett, P.T. Jr. Lansbury, Seeding "one-dimensional crystallization" of amyloid: a
614 pathogenic mechanism in Alzheimer's disease and scrapie? Cell 73 (1993) 1055-1058.
615[47] L. Fu, I. Matsuyama, T. Chiba, Y. Xing, T. Korenaga, Z. Guo, X. Fu, J. Nakayama, M.
616 Mori, K. Higuchi, Extrahepatic expression of apolipoprotein A-II in mouse tissues: possible
617 contribution to mouse senile amyloidosis, J. Histochem. Cytochem. 49 (2001) 739-747.
618[48] G.G. Glenner, Amyloid deposits and amyloidosis. The beta-fibrilloses (first of two parts),
619 N. Eng. J. Med. 302 (1980) 1283-1292.
620[49] A. Andreola, V. Bellotti, S. Giorgetti, P. Mangione, L. Obici, M Stoppini, J. Torres, E.
621 Monzani, G. Merlini, M. Sunde, Conformational switching and fibrillogenesis in the
622 amyloidogenic fragment of apolipoprotein A-I, J. Biol. Chem. 278 (2003) 2444-2451.
623[50] K. Hasegawa, S. Tsutsumi-Yasuhara, T. Ookoshi, Y. Ohhashi, H. Kimura, N. Takahashi, H.
624 Yoshida, R. Miyazaki, Y. Goto, H. Naiki, Growth of β2-microglobulin-related amyloid
625 fibrils by non-esterified fatty acids at a neutral pH, Biochem. J. 416 (2008) 307-315.
626[51] D.P McGowan, W. Van Roon-Mom, H. Holloway, G.P. Bates, L. Mangiarini, G.J. Cooper,
627 R.L. Faull, R.G. Snell, Amyloid-like inclusions in Huntington's disease, Neurosci. 100
628 (2000) 677-680.
629[52] K. Higuchi, J. Wang, K. Kitagawa, T. Matsushita, K. Kogishi, H. Naiki, H. Kitado, M.
630 Hosokawa, Accelerated senile amyloidosis induced by amyloidogenic apoA-II gene
631 shortens the life span of mice but does not accelerate the rate of senescence, J. Gerontol. A

632 Biol. Sci. Med. Sci. 51 (1996) B295-302.

633[53] T. Chiba, K. Kogishi, J. Wang, C. Xia, T. Matsushita, J. Miyazaki, I. Saito, M. Hosokawa,
634 K. Higuchi, Mouse senile amyloid deposition is suppressed by adenovirus-mediated
635 overexpression of amyloid-resistant apolipoprotein A-II, Am. J. Pathol. 155 (1999) 1319-
636 1326.

637[54] J. Suto, Y. Takahashi, K. Sekikawa, Quantitative trait locus analysis of plasma cholesterol
638 and triglyceride levels in C57BL/6J × RR F_2 mice, Biochem. Genet. 42 (2004) 347-363.

639[55] Kumar MS, Carson M, Hussain MM, Murthy HM, Structures of apolipoprotein A-II and a
640 lipid-surrogate complex provide insights into apolipoprotein-lipid interactions, Biochem. 41
641 (2002) 11681-11691.

642[56] Zhang H, Sawashita J, Fu X, Korenaga T, Yan J, Mori M, Higuchi K, Transmissibility of
643 mouse AApoAII amyloid fibrils: inactivation by physical and chemical methods, FASEB J.
644 20 (2006) 1012-1014. Epub 2006 Mar 20.

645[57] Yanagisawa K, Okada A, Suzuki N, Ihara Y, GM1 ganglioside-bound amyloid β-protein
646 (Aβ): a possible form of preamyloid in Alzheimer's disease, Nat. Med. 1 (1995) 1062-1066.

647[58] Y. Tashima, R. Oe, S. Lee, G. Sugihara, E.J. Chamners, M. Takahashi, T. Yamada, The
648 effect of cholesterol and monosialoganglioside (GM1) on the release and aggregation of
649 amyloid β-peptide from liposomes prepared from brain membrane-like lipids, J. Biol.
650 Chem. 279 (2004) 17587-17595.

651[59] H. Hayashi, N. Kimura, H. Yamaguchi, K. Hasegawa, T. Yokoseki, M. Shibata, N.
652 Yamamoto, M. Michikawa, Y. Yoshikawa, K. Terao, K. Matsuzaki, C.A. Lemere, D.J.
653 Selkoe, H. Naiki, K. Yanagisawa, A seed for Alzheimer amyloid in the brain, J. Neurosci.
654 24 (2004) 4894-4902.

655[60] N. Yamamoto, Y. Hirabayashi, M. Amari, H. Yamaguchi, G. Romanov, W.E. Van
656 Nostrand, K. Yanagisawa, Assembly of hereditary amyloid β-protein variants in the

657 presence of favorable gangliosides, FEBS Lett. 579 (2005) 2185-2190.

658[61] M. Molander-Melin, K, Blennow, N. Bogdanovic, B. Dellheden, J.E. Månsson, P. Fredman,
659 Structural membrane alterations in Alzheimer brains found to be associated with regional
660 disease development; increased density of gangliosides GM1 and GM2 and loss of
661 cholesterol in detergent-resistant membrane domains, J. Neurochem. 92 (2005) 171-182.

662[62] M. Zhu, A.L. Fink, Lipid binding inhibits α-synuclein fibril formation, J. Biol. Chem. 278
663 (2003) 16873-16877.

Figure Legends

Figure 1: Amino acid sequences of mouse apoA-II and synthetic partial peptides. Mature apoA-II consists of 78 amino acid residues, and pro-apoA-II has a 5-residue-long propeptide extending from the N-terminus of mature apoA-II. The *encircled words* are amino acids of the propeptide sequence, the **bold words** at position 5 and 38 are the two variant amino acids between type B and C apoA-II. Synthesis of partial peptides was performed from NH_3-terminal side toward COOH-terminal side as the arrowhead. The following arrows show synthetic partial peptides: solid lines, N-terminal peptides; dotted lines, middle part peptides; dashed lines, C-terminal peptides. **Bold** words and lines indicate synthetic peptides capable of amyloid fibril formation.

Figure 2: The unique combination of N- and C-terminal peptides of apoA-II is essential for amyloid fibril formation at pH 2.5. **A**. The left panel shows ThT-fluorescence intensities of the reaction mixtures of N- and C-terminal peptides (c16p + 48/65, 50 μM × 2) at pH 2.5, 4.5, or 7.0. Each symbol and bar represents the mean and S.D. (n = 3). a. u., arbitrary units. The fluorescence intensities of either c16p or 48/65 (300 μM, n = 2) showed minimal increase after 24 h incubation at pH 2.5. The right panel shows the ThT-fluorescence plot of amyloid fibril formation of the c16p + 48/65 peptides following up to 18 h of incubation at pH 2.5, and demonstrates the presence of a lag-time phase. **B**. The reaction mixtures at pH 2.5 had the most abundant amyloid fibrils. Characteristic forms of amyloid fibril were observed in the reaction mixtures after 21 h or 3 days incubation by a negative-staining method using TEM (left-hand panel). The products were stained with Congo-red, and we observed the apple-green color birefringence under polarized light using LM (right-hand panel). Each scale bar in the TEM images indicates 100 nm in

687width. **C**. LC/MS/MS analysis shows a representative profile of c16p + 48/65 mixture
688after 21 h incubation at pH 2.5. Amyloid fibrils formed from peptides have both N- and
689C-terminal peptides in a 1:1 ratio.

690**Figure 3**: Far-UV CD spectra revealed that the combination of c16p and 48/65 peptides
691changed structure greatly and resulted in the abundant formation of amyloid fibrils under
692the acidic conditions. **A**. The far-UV CD spectrum of c16p + 48/65 during immediate
693phase shows a similar profile to that of the c16p peptide rather than the merged curve of
694each spectrum of c16p and 48/65 (dashed line). The spectrum of these peptides incubated
695for 12 h at 37˚C at pH 2.5 (overnight phase) changed greatly and exhibited one broad and
696negative peak at 216 nm. Results are expressed in terms of means residue ellipticity
697(MRE). **B**. The CD spectra of the c16p + 48/65 peptides during immediate phase (*left*
698*panel*) and incubated for 12 h at 37˚C (overnight phase) at pH 4.5 and 7.0 were shaped
699differently to the curves at pH 2.5.

700**Figure 4**: The Gln at position 16 of apoA-II plays an indispensable role in amyloid fibril
701formation. Abbreviations and amino acid sequences of N-terminal peptides used are
702shown in **Fig. 1**. Each symbol and bar represents the mean and S.D. (n = 3). a. u.,
703arbitrary units. **A**. ThT-fluorescence intensities of each reaction mixture of N-terminal
704peptides (c1/16, c2/16, or 6/16) and 48/65 increased as well as those of c16p + 48/65. The
705fluorescence intensities of 9/16 without amino acids at positions 1–8 and 48/65 increased
706only slightly. **B**. The fluorescence intensities of each reaction mixture of N-terminal
707peptides without amino acids at positions of 9–16 or 14–16 (c8p or c13p) and 48/65 did
708not increase. **C**. The fluorescence intensities of each reaction mixture of N-terminal
709peptides without an amino acid at position 16 (c15p) and 48/65 increased less than c16p +

71048/65. The fluorescence intensities of the reaction mixture of the N-terminal peptides 711with His substituted for Gln at position 16 (c1/16(Q16H)) and 48/65 decreased compared 712to c1/16 + 48/65. **D**. The fluorescence intensities of each reaction mixture of reverse 713synthetic peptides (16/6 or 65/48) did not change. **E**. The reaction mixtures of N-terminal 714peptides (c1/16, c2/16, or 6/16) and 48/65 after 20 or 21 h incubation had the most 715abundant amyloid fibrils, and the mixtures of c1/16(Q16H) and 48/65 after 21 h 716incubation had fewer amyloid fibrils. Characteristic forms of amyloid fibril were not 717detected in either reaction mixture of other N-terminal peptides (9/16 or c15p) with 48/65 718and reverse-reverse combination (6/16 and 65/48) after 20 or 21 h incubation using TEM. 719Each scale bar indicates 100 nm in width.

720**Figure 5**: N-terminal peptides of type B and 48/65 polymerize into amyloid fibrils in a 721similar fashion as type C. **A**. This panel shows ThT-fluorescence intensities of b16p + 72248/65 mixture (50 μM × 2) at pH 2.5, 4.5, or 7.0. Those fluorescence intensities increased 723like the intensities of type C (c16p) and 48/65 shown in **Fig. 2A**. Each symbol and bar 724represents the mean and S.D. (n = 3). a. u., arbitrary units. **B**. The reaction mixtures of 725type B peptides at pH 2.5 had the most abundant amyloid fibrils. Characteristic forms of 726amyloid fibril observed in the reaction mixtures after 21 h or 3 days incubation using 727TEM are shown in the left panel. After 3 days the products were stained with Congo-red, 728and the apple-green color birefringence under the polarized light using LM is shown in the 729right panel. Each scale bar in the TEM image indicates 100 nm in width.

730**Figure 6**: The C-terminal peptide (48/65) is indispensable but middle part peptides 731(32/43) have no effect in amyloid fibril formation. Abbreviations and amino acid 732sequences of C-terminal and middle part peptides used are shown in **Fig. 1**. Each symbol

733and bar represents the mean and S.D. (n = 3). a. u., arbitrary units. **A**. ThT-fluorescence 734intensities of the reaction mixtures of c16p and each shorter peptides of 48/65 (48/57 + 73556/65, 48/57, 52/61, or 56/65), or another C-terminal peptide (64/78) increased less than 736c16p + 48/65 at pH 2.5. **B**. The fluorescence intensities of the reaction mixtures of middle 737part peptide (c32/43) and either c16p or 48/65 (c16p + c32/43 or 48/65 + c32/43) did not 738increase compared with those of c16p + 48/65 at pH 2.5. The fluorescence intensities of 739the reaction mixtures of c16p, 48/65, and c32/43 (c16p + 48/65 + c32/43) increased 740similar to c16p + 48/65. **C**. The fluorescence intensities of b16p and 48/65 with or 741without b32/43 (b16p + 48/65 + b32/43 or b16p + 48/65) increased similar to those of 742type C peptides shown in panel B.

743**Figure 7**: Seed-dependent amyloid fibril extension of type B and C peptides. N-terminal 744peptides can polymerize into amyloid fibrils in the presence of seeds even without the C-745terminal peptide. Each symbol and bar in panels **A-C** represents the mean and S.D. (n = 7463). a. u., arbitrary units. **A**. In the presence of pre-made amyloid fibrils of type C 747peptides, the ThT-fluorescence intensities of type C N-terminal peptides (c16p and c1/16) 748and 48/65 increased from the beginning of incubation, and reached a plateau phase after 749approximately 2 h. The fluorescence intensities of type B N-terminal peptide (b16p) and 75048/65 increased similarly without a lag-time phase. However, the fluorescence intensities 751of shorter N-terminal peptides (c8p and c13p) and 48/65 showed little increase. The right 752panel demonstrates the ThT-fluorescence plot of c16p + 48/65 without a lag-time (seeds 753(+)). **B**. In the presence of type B pre-made amyloid fibrils, the fluorescence intensities of 754type B or C peptides also increased without a lag-time phase. **C**. In the presence of type C 755seeds, the fluorescence intensities of the reaction mixture of c16p even without 48/65

gradually increased, but those of 48/65 alone (48/65) did not. **D**. TEM images of the type C mixtures after 3 days incubation. The reaction mixtures of type C seeds without peptides had no amyloid fibrils (Seed alone), but the reaction mixtures of c16p and 48/65 in the presence of seeds had abundant amyloid fibrils (c16p + 48/65). Narrow and bent fibrils were detected as well as characteristic forms of amyloid fibril in the reaction mixtures of c16p without 48/65 (c16p). The reaction mixtures of 48/65 alone had no amyloid fibrils (48/65). Each scale bar in TEM image indicates 100 nm in width.

Figure 8: A hypothetical mechanism of AApoAII amyloid fibril formation in vitro and in vivo. **A**. A presentation of structural states and amyloid fibril formation of apoA-II peptides in vitro. Neither N- nor C-terminal peptides polymerize into amyloid fibrils independently (1). Combination of N- and C-terminal peptides under acidic conditions (pH 2.5) makes intermediates with increased unordered structures (amyloidogenic conformation), which are favored in amyloid nucleus formation (2). Once a nucleus is formed, or preformed nuclei (seeds) are added, further extension of N- and C-terminal peptides occurs (3). In the presence of 'nuclei or seeds', the N-terminal peptide polymerizes into amyloid fibrils even without the C-terminal peptide (4), but the C-terminal peptide alone does not (5). **B**. A hypothesis of apoA-II amyloid fibril formation in vivo. ApoA-II generates surface patches that associate with lipids in HDL particle. ApoA-II is detached from the lipid surface by unknown environmental factors, takes unfolded structure and polymerizes into amyloid fibrils by the combination of N- and C-amino acid sequences. Invasion of exogenous AApoAII amyloid fibrils induces extension step and accelerates amyloidosis.

Figure S1: Characteristic forms of amyloid fibril were increased until they reached a

779plateau phase after 6 h incubation at pH 2.5. Each scale bar in the images indicates 100
780nm in width.

781Methods: Reaction mixtures in ice-cold Eppendorf tubes contained 50 μM synthetic
782peptides (c16p + 48/65 (**A**) or b16p + 48/65 (**B**)), 50 mM citrate buffer (pH 2.5), 100 mM
783NaCl, and 5% DMSO as a final concentration. After brief blending, the reaction mixtures
784were incubated with agitation at 300 rpm in a shaker at 37˚C. Aliquots of the reaction
785mixtures were spread on carbon-coated grids, and were negatively stained with 1%
786phosphotungstic acid–NaOH (pH 7.0). These samples were examined under an electron
787microscope (1200 EX, JEOL, Tokyo, Japan) with an acceleration voltage of 80 kV.

788**Figure S2**: ThT-fluorescence intensities of the reaction mixtures of type C N- and C-
789terminal peptides were increased under strong-acidic conditions. Each symbol represents
790the mean ± S.E. (n = 6). a. u., arbitrary units.

791Methods: Reaction mixtures in an ice-cold tubes contained 50 μM synthetic peptides
792(c1/16 and 48/65), 50 mM reaction buffer, 100 mM NaCl, and 5% DMSO as final
793concentration. Reaction buffers used were sodium citrate buffer (pH 2.5-6.0, closed
794circle) or sodium phosphate buffer (pH 6.0-7.4, open circle). After brief blending, the
795reaction mixtures were incubated with agitation at 300 rpm in a shaker at 37˚C for 20 h,
796and were used for ThT binding assay. ThT binding assay was performed as described in
797the **Materials and methods**.

798**Figure S3**: The characteristic forms of amyloid fibril were detected in the reaction
799mixture of c16p and 48/65 in a 5:1 ratio, but somewhat different shapes were revealed. **A**.
800The left panel shows ThT-fluorescence intensities of the reaction mixtures of c16p +
80148/65 (1:1, closed circle; 5:1, open square) at pH 2.5. Each symbol and bar represents the

802mean and S.D. (n = 3). a. u., arbitrary units. The right panel shows the ThT-fluorescence 803plot of amyloid fibril formation of the c16p + 48/65 peptides following up to 8 h of 804incubation at pH 2.5, and demonstrates the presence of a lag-time phase. **B**. LC/MS/MS 805analysis shows a representative profile of c16p + 48/65 mixture after 21 h and 3 days of 806incubation at pH 2.5. **C**. Characteristic forms of amyloid fibril were observed in the 807reaction mixtures after 3 days of incubation by a negative-staining method using TEM. 808Somewhat narrow and curving amyloid fibrils were observed (arrow head). The scale bar 809indicates 100 nm in width.

810Methods: Reaction mixtures contained c16p + 48/65 in the ratio of either 50 μM × 2 (1:1) 811or 250 μM + 50 μM (5:1), 50 mM citrate buffer (pH 2.5), 100 mM NaCl, and 5% DMSO 812as a final concentration. After brief blending, the reaction mixtures were incubated with 813agitation at 300 rpm in a shaker at 37˚C. Aliquots were used for ThT binding assay, LC/ 814MS/MS and TEM at arbitrary intervals. Those assays were performed as described in the 815**Materials and methods**.

816

J. Sawashita *et. al.* **Figure 1**

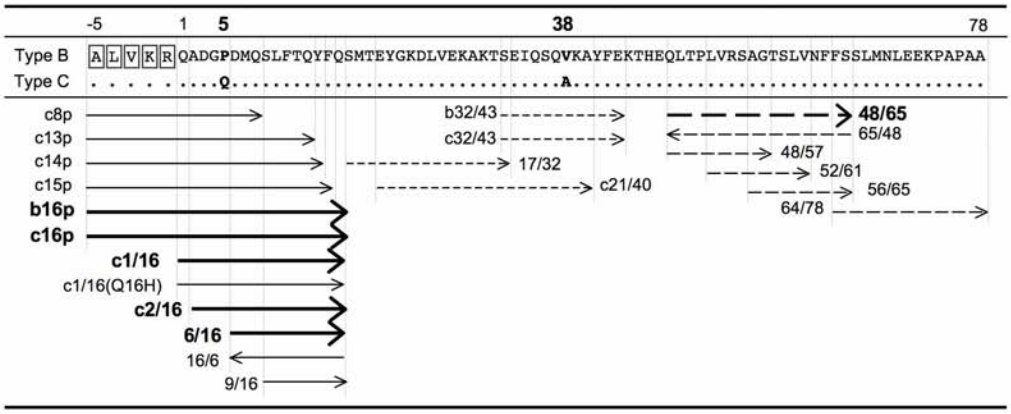

818

J. Sawashita *et. al.* **Figure 2**

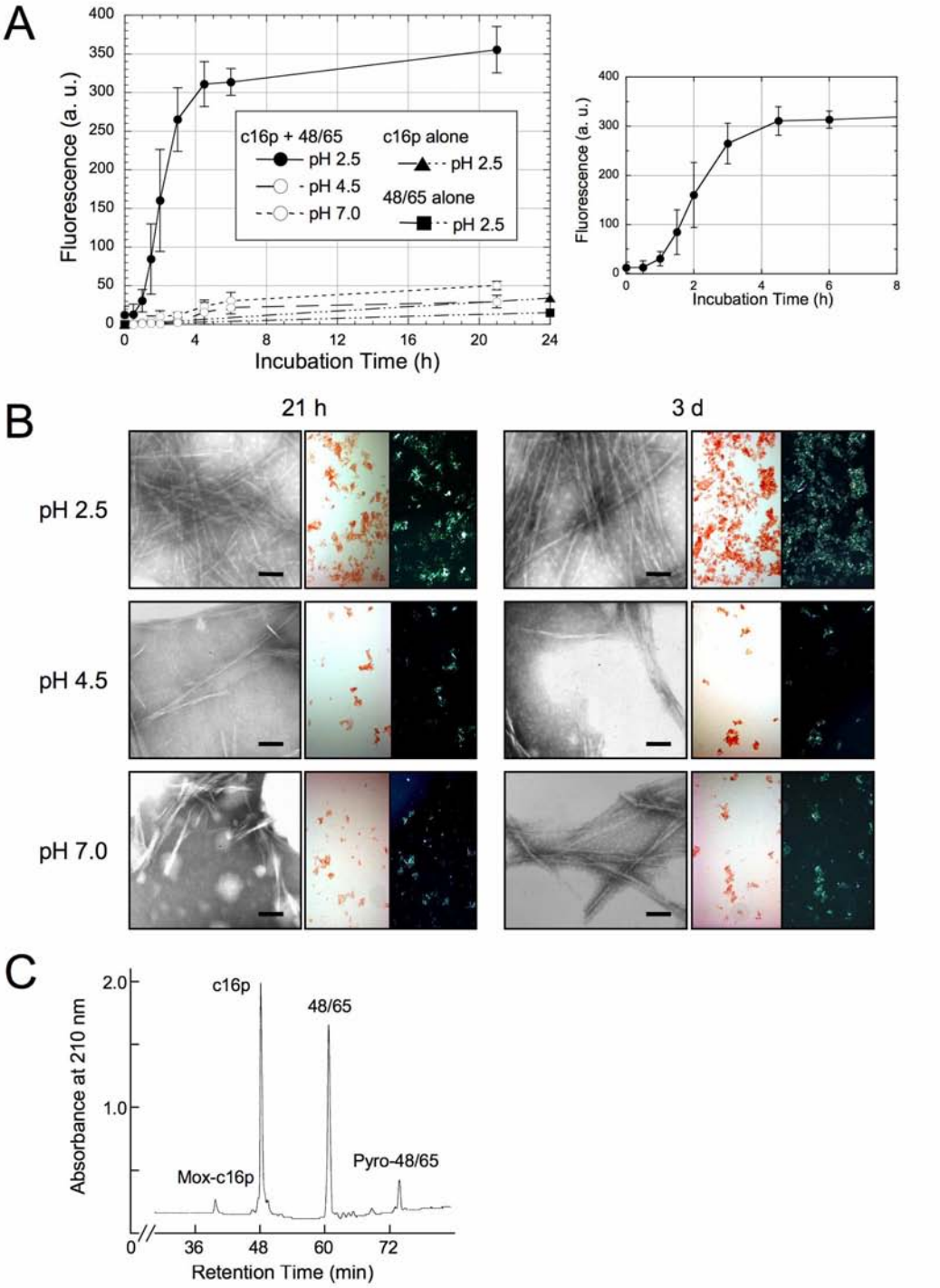

820

J. Sawashita *et. al.* **Figure 3**

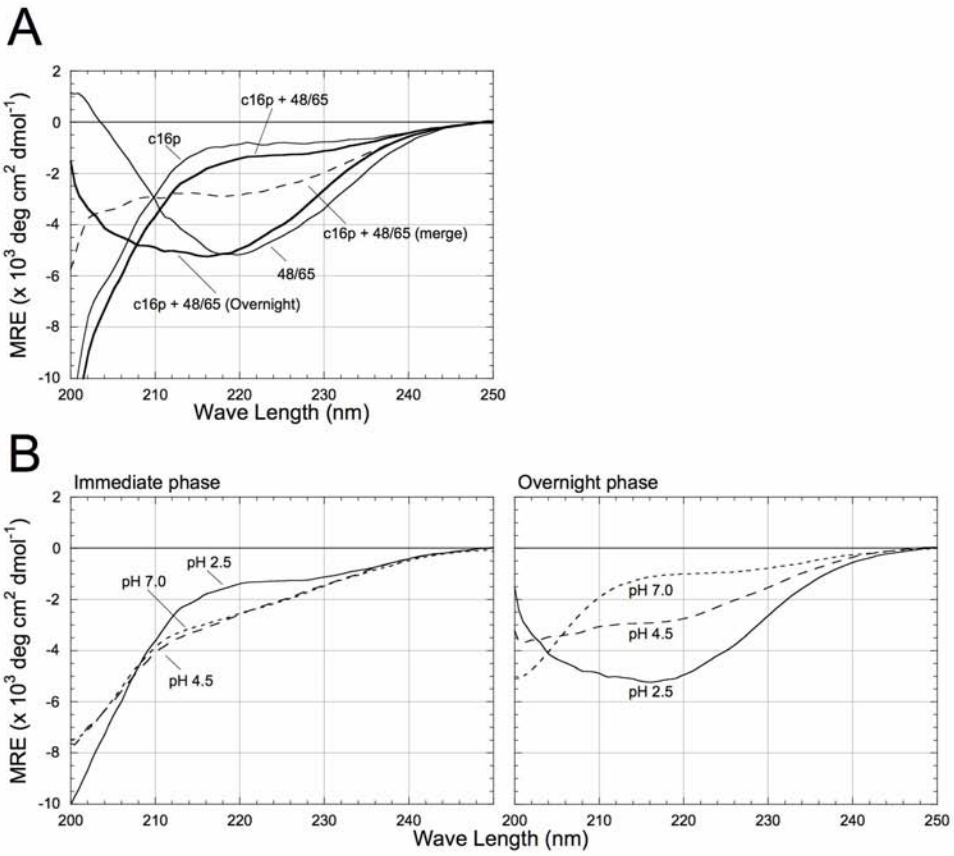

822

J. Sawashita *et. al.* **Figure 4**

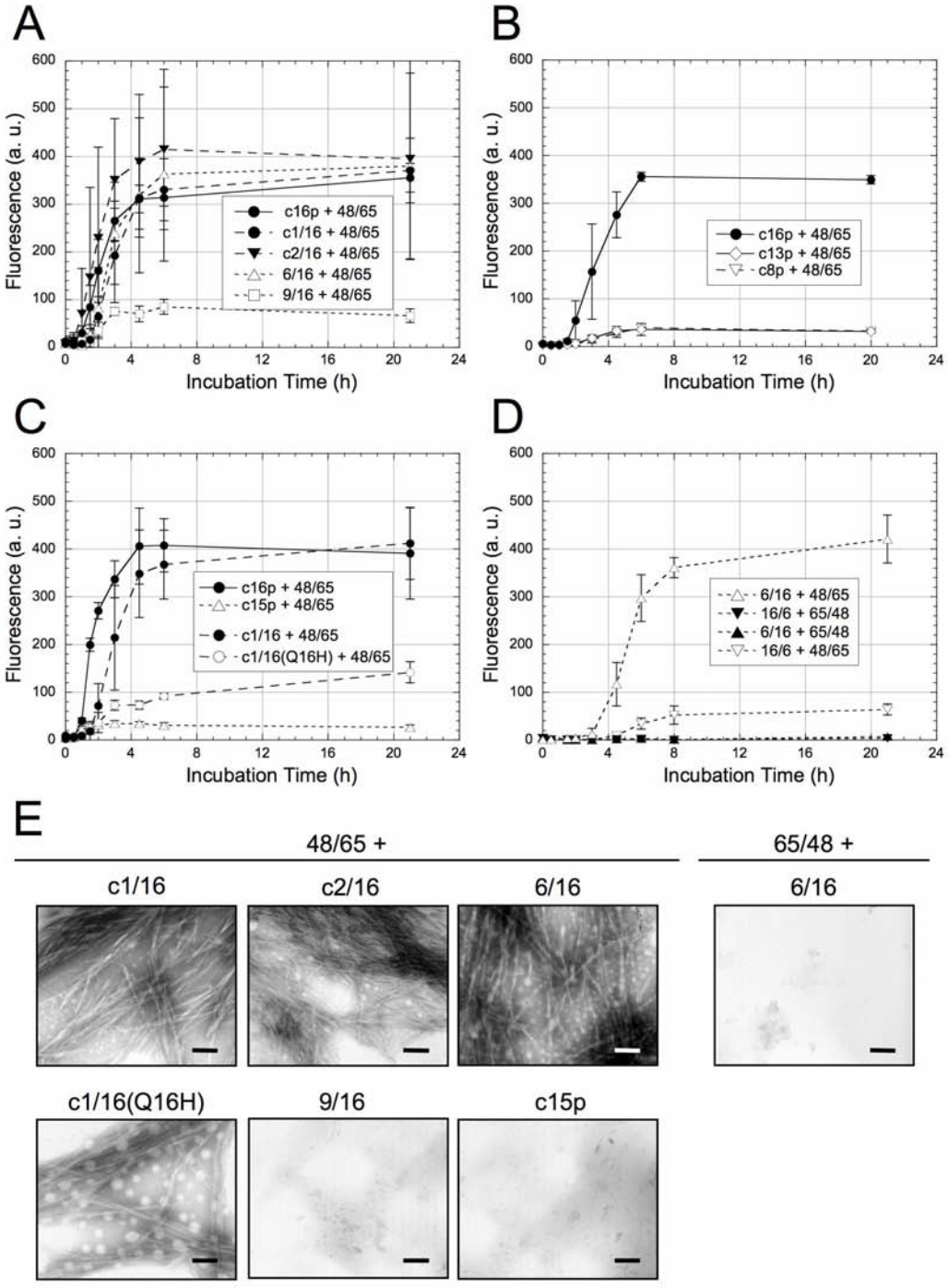

824

J. Sawashita *et. al.* **Figure 5**

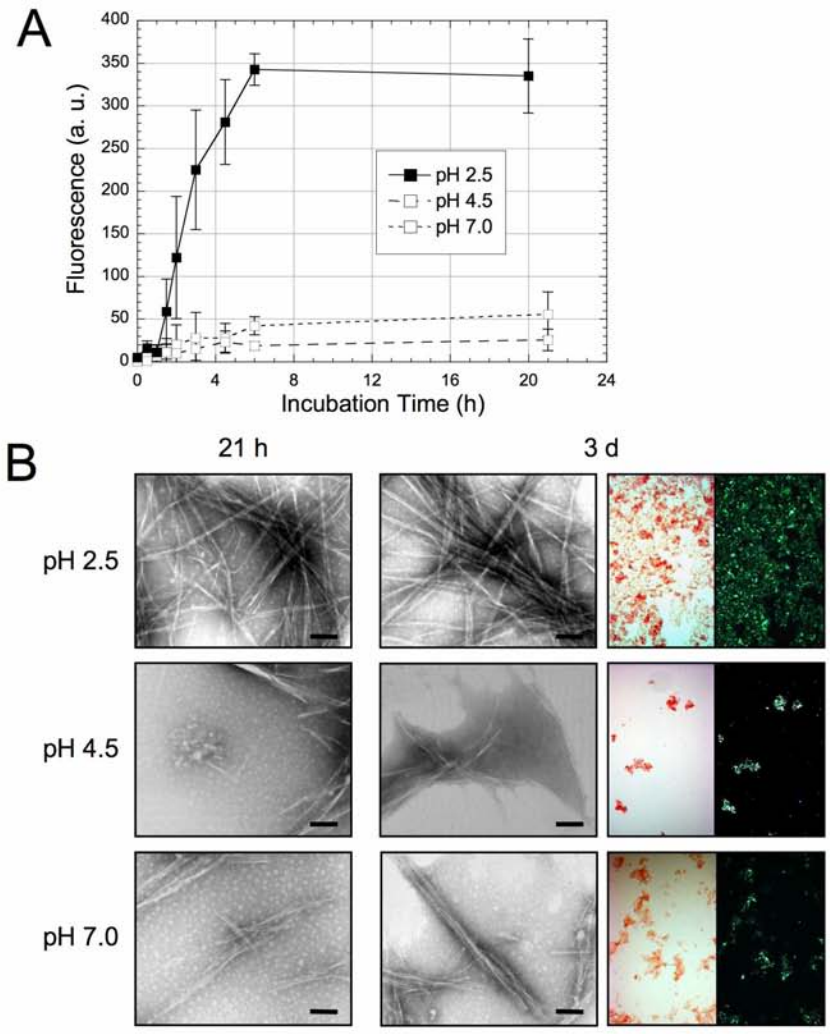

826

J. Sawashita *et. al.* **Figure 6**

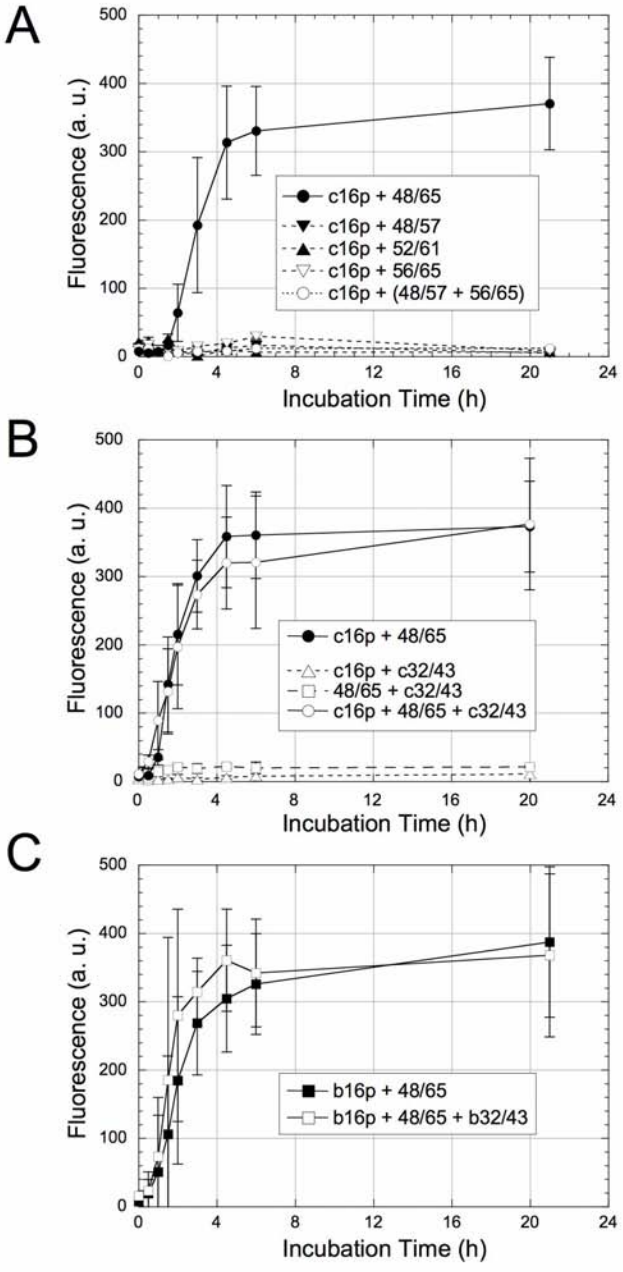

828

J. Sawashita *et. al.* **Figure 7**

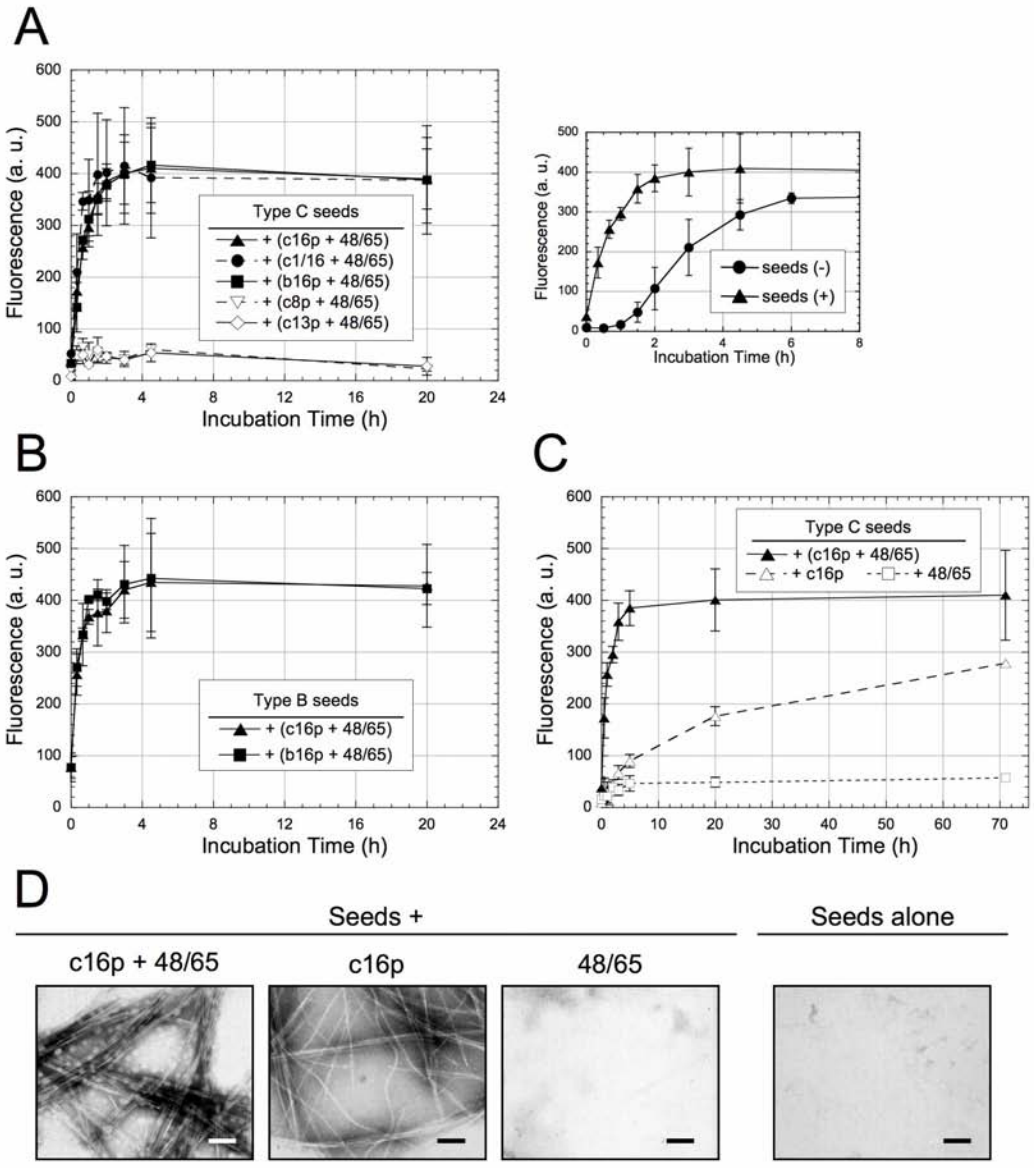

830

J. Sawashita *et. al.* **Figure 8**

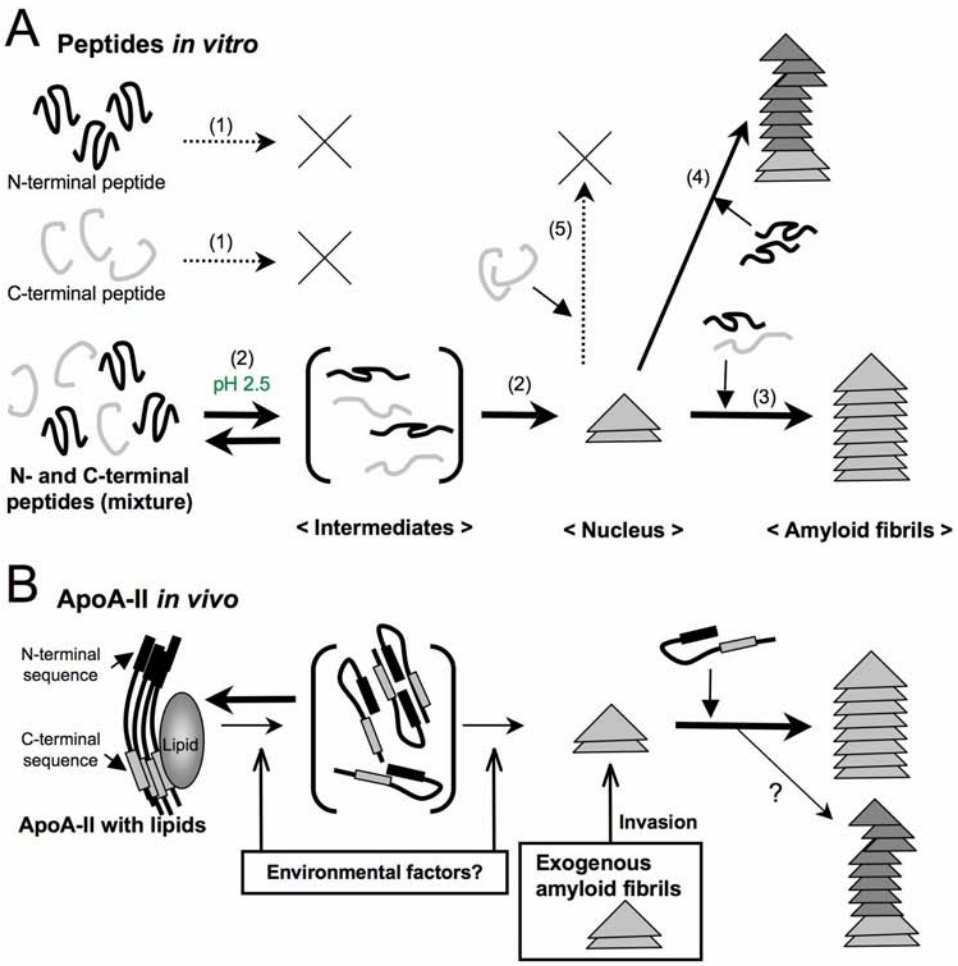

137 46

138